2016 IEEE International Conference on Advanced Intelligent Mechatronics (AIM)
Banff, Alberta, Canada, July 12–15, 2016

Experimental Studies on Q filter Design of a Disturbance Observer for a One-wheel Robot

S. D. Lee and S. Jung, *Member, IEEE*

***Abstract*—In this paper, experimental studies on designing Q filters in the disturbance observer (DOB) based motion control for balancing a one-wheel robot are presented. The robot is simply modeled as a second order system and the corresponding Q filters are designed to form a DOB control structure. Two Q-filters such as Q20 and Q31 are investigated and analyzed in a view point of disturbance rejection performance and sensor noise immunity. The performances of two Q filters are evaluated by realizing a DOB in the digital system for controlling the balance of a single-wheel mobile robot.**

***Index Terms*— DOB, one-wheel robot, Q-filter design.**

I. Introduction

ACTUATOR shortage often makes a system unstable so that control of underactuated systems is difficult and challenging. Two-wheel mobile robots are a typical underactuated system of which control are quite challenging [1-3]. Two-wheel mobile robots have been commercialized as a personal transportation system.

Beyond two-wheel mobile robots, a one-wheel mobile robot has an extreme structure of nonhononomic systems that have only a single wheel to maintain balance as well as to navigate in its terrain. For the balancing control of the robot, a direct actuator is used for driving and an indirect actuator called CMG (Control Moment Gyro) for balancing [4,5].

In order for the CMG to work properly, the flywheel of CMG must maintain its angle within a controllable boundary when the gyroscopically induced yawing motion for the posture control is utilized. It is found from our previous experiences that a yaw-dominant(gyroscopically induced) force is diminished when the position of the flywheel goes over 45 degrees in the direction of the tilting axis [6,7]. This results in the instability of the robot.

Therefore, the actuator of the robot must be controlled considering three motions simultaneously in the system. Three motions to induce the gyroscopic effect are required to be stable and decoupled for the better performance. Therefore, it is possible to attain a goal of using one actuator and one sensor architecture when the overall disturbances are minimized.

In order to deal with disturbances in the control system, many control methods have been proposed in the literature [8-23]. Adaptive control and robust control for nonlinear systems have been proposed [8,9]. DOB has been used intensively for the motion control area [10-23]. DOB is one of robust control methods that provide a cost-effective solution for the sensor-less control [10,11].

One practical aspect of DOB can treat the difference between a real and a nominal model as a disturbance. In a single-wheel robot system, overall uncertainties such as ground friction of robot system, pulley-belt perturbation of gimbal system, vibration of high imbalanced flywheel, model uncertainty, and control signal distortion can be considered as disturbances in the DOB control structure.

When DOB is applied to the system, decoupled control is possible as a result since all the disturbances of the system are removed by the DOB. DOB should deal with a trade-off between the disturbance rejection performance and the sensor noise immunity. It is well known that a lowpass filter called Q filter is preferred to satisfy both specifications.

In the framework of Q filter design, three well-known methods have been proposed. Ohnishi [19], Umeno [20], and Tomizuka [21] have been proposed guidelines for various Q-filter designs. In this paper, we design a Q-filter following Tomizuka.

Therefore, in this paper, the characteristics of Q filters in the DOB-based control of a single-wheel robot are addressed. Firstly, a nominal model of a single-wheel robot is derived as a second order inverted stick model. Secondly, the bound of the time constant of Q-filter is analyzed. Two Q-filters such as Q20 and Q31 are analyzed for the disturbance rejection performance and sensor noise immunity. Lastly, experiments are conducted to compare the performances by Q filters .

II. Mechanism and Modeling

A. Actuator mechanism

A one-wheel robot system is shown in Fig.1, where CMG is utilized for generating a gyroscopic effect on the body system. The gyroscopic torque can be formed in the direction of the cross product between the angular momentum of the high rotating flywheel and the rotating tilt motion. The induced gyroscopic torque is described as

This work has been supported by the 2014 basic research funds through the contract of National Research Foundation of Korea (NRF-2014R1A2A1A11049503).

S. D. Lee and S. Jung are with Department of Mechatronics Engineering, Chungnam National University, Daejeon, Korea 305-764 (e-mail: jungs@cnu.ac.kr).

$$\boldsymbol{\tau} = \mathbf{H} \times \boldsymbol{\Omega} \quad (1)$$

where, $\boldsymbol{\tau}$(Nm) is the gyroscopic torque, $\mathbf{H}$(Nms / rad) is the angular momentum of the high rotating flywheel, and $\boldsymbol{\Omega}$(rad / s) is the tilt rate of the gimbal system.

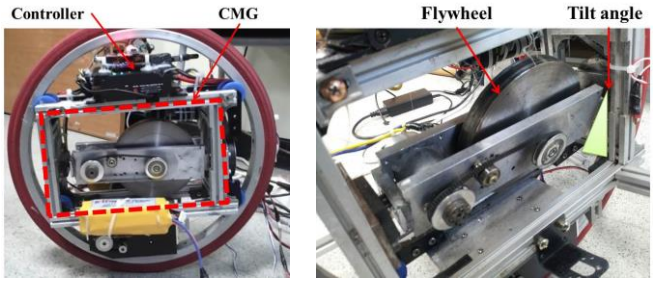

(a) Robot system (b) CMG

Fig. 1 Robot and actuator

In equation (1), the gyroscopic torque of the body system is dependent both on the magnitude of an angular momentum and a tilt rate. The direction of the torque is dependent on the tilt motion. The expected direction of the gyroscopic torque is the yaw and pitch directions of the body system. When the tilt angle is maintained within a small angle, the yaw angle can be the major direction of the induced torque.

However, when the tilt angle is over 45 degrees, the major direction of the toque can be a pitch. Therefore, the tilt angle must be maintained within a limited boundary during the posture control of a body system. It is one of the problems of a one-wheel system.

As a posture control mechanism, we use the yaw direction torque. When the body leans toward one side, the yawing torque can be applied to the body system where the ground friction prohibits the robot from moving toward the yaw direction only. Conflict between the yawing torque and the friction generates a rolling effect of the body system. However, the ground friction is dependent on the natural force of a mass system. This results in a limited value.

Therefore, lateral control such as roll angle control of the body system is strongly dependent on the yawing angle control of the system where uncertain frictional force is combined. In addition, the yawing motion of the body system is strongly related with the tilt angle of CMG where the pulley-belt mechanism for the tilt motion may generate unexpected disturbances [22,24].

There are three control problems such as a tilt angle of the flywheel, a yaw angle of the body, and a roll angle of the body. If all the disturbances and frictions are neglected in the system, three variables have linear relationships. The properly controlled tilt angle generates a proper yawing torque, and then the proper yawing torque is transferred regularly to the rolling torque in that condition.

B. *Dynamic model*

When overall disturbances are assumed to be neglected, the dynamic model of the system can be modeled as an inverted stick model. The center of mass is placed at the half of the stick length. Only the roll motion θ and $\dot{\theta}$ are used. The direction of the gyroscopic torque is the direction of θ .

Under the high rotating inner flywheel condition of the system, estimating I is not easy to solve. As one of solutions for it, experimental results are used [24].

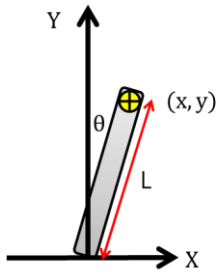

Items	Definitions	Values	Units
L	A length	0.5	m
M	Mass	12	Kg
I	Estimated moment of inertia of the flywheel	7.5	kgm^2
g	Gravity acceleration	9.8	ms^{-2}

Fig. 2 Model coordinates and parameter specifications

(x, y) as a function of roll angle is described.

$$x = L\sin\theta\ ,\ y = L\cos\theta \quad (2)$$

$$\dot{x} = L\dot{\theta}\cos\theta\ ,\ \dot{y} = -L\dot{\theta}\sin\theta \quad (3)$$

Total kinetic energy is a sum of kinetic energies from a wheel and a flywheel.

$$T = \frac{1}{2}ML^2\dot{\theta}^2 + \frac{1}{2}I\dot{\theta}^2 \quad (4)$$

where I is the moment of inertia of the high rotating flywheel. Potential energy is

$$V = MgL\cos\theta \quad (5)$$

The Lagrangian formulation is given

$$L = T - V = \frac{1}{2}(ML^2 + I)\dot{\theta}^2 - MgL\cos\theta \quad (6)$$

Therefore, torque dynamics can be shown as

$$\frac{d}{dt}\left(\frac{\partial L}{\partial \dot{\theta}}\right) - \frac{\partial L}{\partial \theta} = (ML^2 + I)\ddot{\theta} - \mathrm{MgLsin}\ \theta = \tau \quad (7)$$

After plugging values for the parameters in Fig. 2, we have the simple dynamic equation.

$$\tau = 10.5\ddot{\theta} - 58.5\sin\theta \quad (8)$$

C. *Model property analysis*

(7) shows a robot dynamics. When θ is maintained within a narrow angle, a simplified model can be obtained as

$$\tau = 10.5\ddot{\theta} - 58.5\theta \quad (9)$$

In (9), θ is 1 degree and $\dot{\theta}$ is 10 degrees per second. The phase trajectory can be analyzed as in Fig. 3.

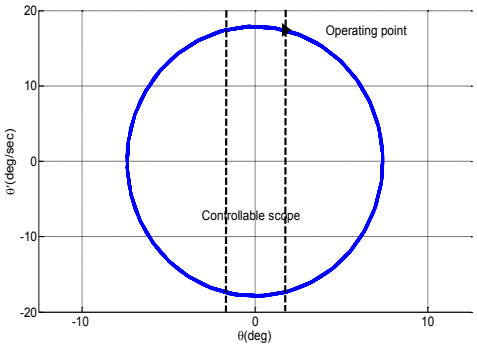

Fig. 3 Trajectory property of the model

Though it shows a semi-stable property, in some conditions such as θ or $\dot{\theta}$ are exceeding the desired level of their position and velocity, it cannot stay in a controllable scope. When we use the PD-controller, the equation can be

$$Kp\,\theta_e + Kd\,\dot{\theta}_e = 10.5\ddot{\theta} - 58.5\theta \qquad (10)$$

where the controller gains, $K_p = 4, K_d = 0.4$ are used.

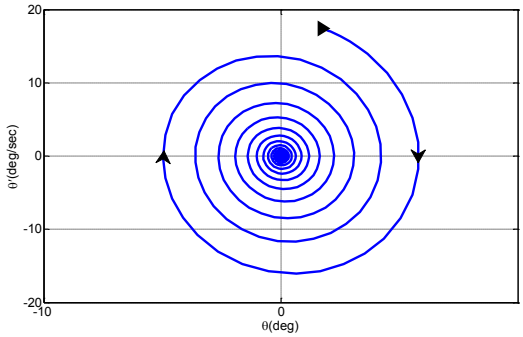

Fig. 4 PD controller effect

We can see the effect of the linear PD-controller in Fig. 4 where the lateral angle shows a converging phenomenon like Fig. 5

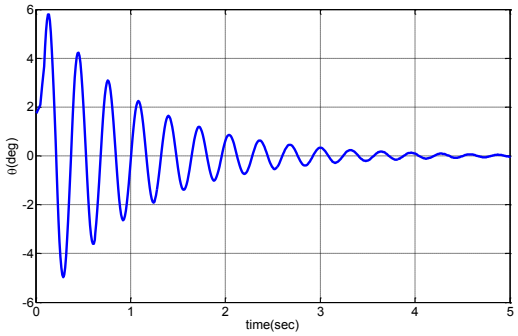

Fig. 5 Converging phenomenon

Surely, a PD-controller is an effective method for the posture control of the proposed model. However, in the real system, the robot may not work as expected. There are many uncertainties in the system.

As a proper analysis of the problem, a sinusoidal disturbance of the function as $5\sin(2\pi 0.5t)$ to the PD-controller in the model is added as shown in Fig. 6. Unlike Fig. 4 and 5, it shows an unknown instability property in the analysis. Moreover, θ and $\dot{\theta}$ go to high position and velocity. Disturbance such as a sinusoidal signal may cause the instability of the system.

Therefore, a DOB based control method is used to compensate for uncertainties in the system.

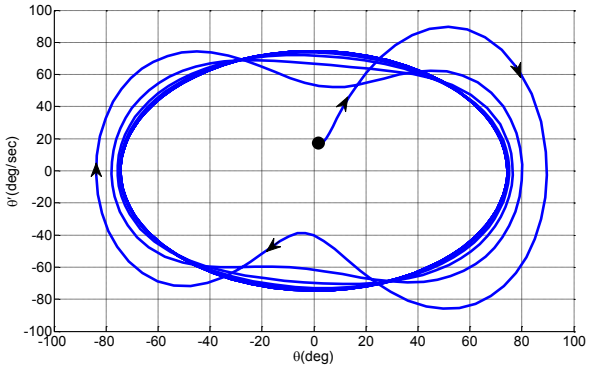

Fig. 6 Disturbed PD-controller effect

D. Q-filter design

The DOB control structure is shown in Fig. 7. In Fig. 7, r is the command input, v is the torque input, u is the disturbance compensated torque input, d is the disturbance, ε is the sensor noise, $\hat{d}$ is the estimated disturbance. The outer loop is the PD-control loop and the inner loop is the disturbance compensator.

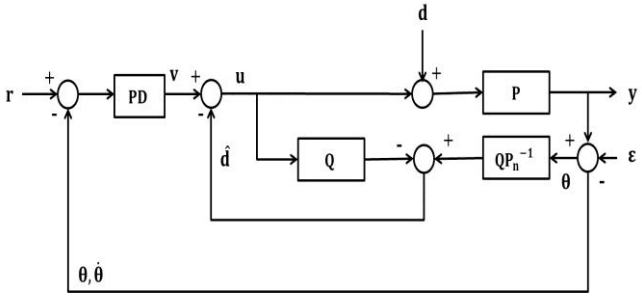

Fig. 7 DOB based control system

When we replace (10) with Laplace transform, we get

$$U(s) = 10.5s^2\theta(s) - 58.5\theta(s) \qquad (11)$$

Therefore, its transfer function can be written as follow.

$$P_n(s) = \frac{\theta(s)}{U(s)} = \frac{1}{10.5s^2 - 58.5} = \frac{0.095}{s^2 - 5.57} \qquad (12)$$

After defining the nominal model of the system as (12), we then design a Q-filter for the DOB. Q-filter can be designed as follows.

$$Q_{mn} = \frac{1 + \sum_{r=1}^{n} C_{mr} (\tau s)^r}{1 + \sum_{r=1}^{m} C_{mr} (\tau s)^r} \tag{13}$$

where, coefficient C_{mr} can be determined as

$$C_{mr} = \frac{m!}{r!(m-r)!} \tag{14}$$

Since the inverse of (12) cannot be realized in the real system, $Q20$ and $Q31$ filters are used as shown below.

$$Q_{20} = \frac{1}{(\tau s)^2 + 2(\tau s) + 2} \tag{15}$$

$$Q_{31} = \frac{3(\tau s) + 1}{(\tau s)^3 + 3(\tau s)^2 + 3(\tau s) + 1} \tag{16}$$

where time constant τ is a design factor.

To select a suitable time constant, its property and sampling rate of the digital system is considered for the control. The sensor feedback and the periodic control loop are done every 0.01s. Therefore, the minimum value of the time constant can be 0.01s. As an upper limit, the natural frequency is considered as follows.

$$\omega_n^{\ 2} = 5.57 (\text{rad}/s) \tag{17}$$

$$f_n = 0.88 (s^{-1}) \tag{18}$$

Therefore, we consider time constant criteria as

$$0.01 < \tau < 1.13 \ (s) \tag{19}$$

The Q-filter characteristic by the time constant is investigated. In Fig. 8, when the time constant is small, the disturbance rejection bandwidth become larger.

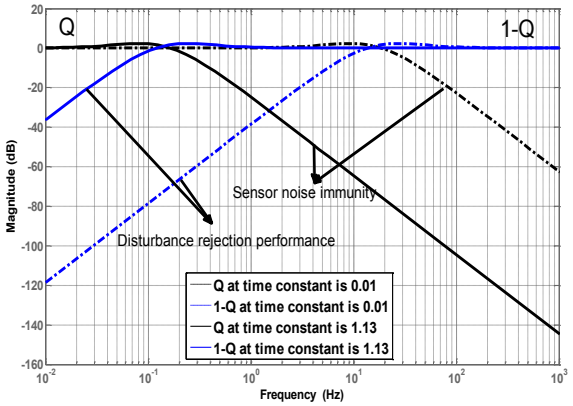

Fig. 8 Q-filter characteristics with time constant

However, in the paper, the performance comparison between Q20 and Q31 is only considered when the time constant is 0.2.

$$Q_{20} = \frac{1}{(0.2s)^2 + 2(0.2s) + 2} \tag{20}$$

$$Q_{31} = \frac{3(\tau s) + 1}{(0.2s)^3 + 3(0.2s)^2 + 3(0.2s) + 1} \tag{21}$$

Then we have

$$P_n^{-1} Q_{20}(z) = \frac{263.2z^2 - 526.1z + 262.8}{z^2 - 1.902z + 0.9048} \tag{22}$$

$$P_n^{-1} Q_{31}(z) = \frac{789.5z^3 - 2354z^2 + 2338z - 774.3}{z^3 - 2.854z^2 + 2.715z - 0.8607} \tag{23}$$

III. Experimental Studies

A. Experimental setup

Two experiments for Q20 and Q31 are conducted. As an experimental setup shown in Fig. 9, we gather the robot posture data through the logger. In the robot, we add an additional sensor to gather the tilt angle data of the robot through RS232 communication which is connected with a PC.

Three control signals such as roll angle and yaw angle of the body, and the tilt angle of the flywheel are also gathered. Body posture such as roll and yaw can be logged every 10ms and the flywheel position such as tilt angle can be logged every 100ms considering the performance of DSP.

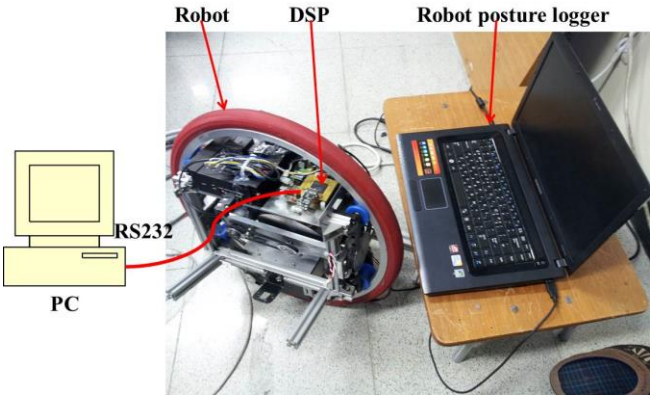

Fig. 9 Experimental setup

B. Balancing control without DOB

Firstly, the balancing control by a PD control method is conducted. Fig. 10 shows the angle responses. The roll angle shows a stable property but the yaw angle goes toward unstable state without returning to the direction of the signal. It leads to the instability of the system and results in falling down on the ground.

Uncertainties in the system may generate imbalance vibration and invoke unknown disturbances at the pulley-belt system of the gimbal system.

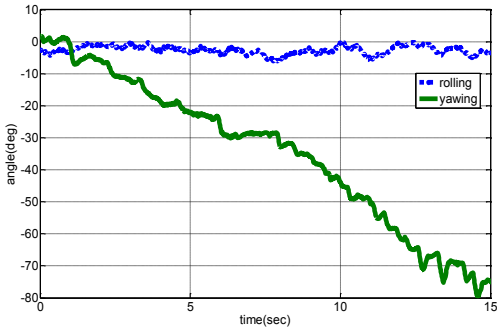

Fig. 10 Experimental result-without DOB

C. *Balancing control with DOB*

DOB effect can be verified through an experiment. Performances of both Q filters are tested and their results are plotted and compared in Fig. 11. Fig. 11 (a) shows the roll angle performance. It is difficult to differentiate the performance between the filters. However, the performance difference can be differentiated from the yaw angle and the gimbal angle shown in Fig. 11 (b) and (c), respectively. From the plots in Fig. 11, the performance of Q20 shows better result than that of Q31.

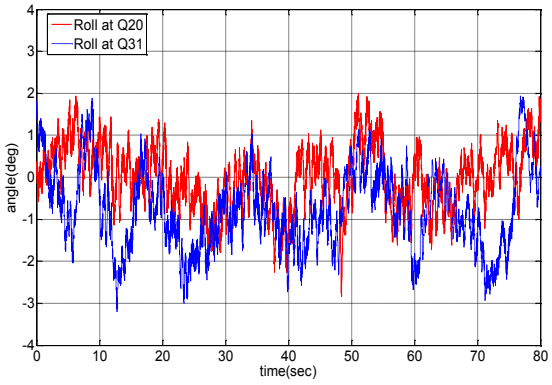

(a) Roll angle

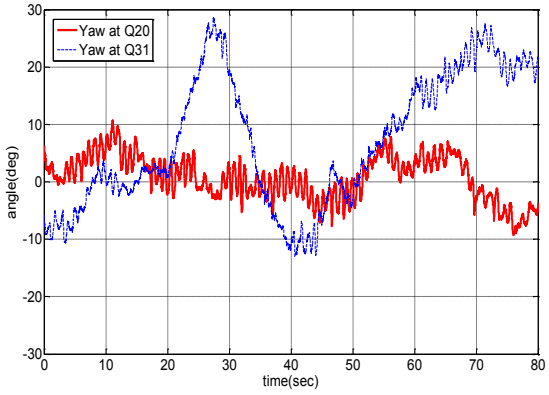

(b) Yaw angle

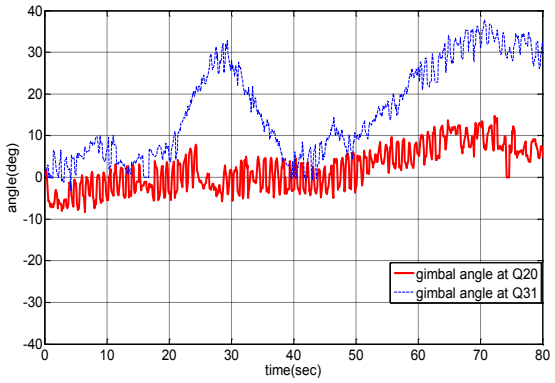

(c) Gimbal angle

Fig. 11 Experimental result with DOB

IV. Conclusion

Q filter design is a crucial factor for the performance of DOB-controlled systems. For the balancing control of a single-wheel robot, DOB performances between Q20 and Q31 are investigated in the paper. Based on the inverted stick model, the system is modeled and analyzed. Through experimental studies, DOB shows the better performance in yaw stabilization than that of a PD control method itself. Between the performances by Q filters, it turned out that Q20 showed a better performance in this typical application. However, other time constants should be considered to generalize the results.

References

[1] K. Pathak, J. Franch, and S. Agrawal, "Velocity and position control of a wheeled inverted pendulum by partial feedback linearization", *IEEE Trans. on Robotics*, vol. 21, pp. 505-513, 2005

[2] S. H. Jeong and T. Takayuki "Wheeled inverted pendulum type assistant robot: design concept and mobile control", *IEEE IROS*, pp. 1932-1937, 2007

[3] S. S. Kim and S. Jung, "Control experiment of a wheel-driven mobile inverted pendulum using neural network", *IEEE Trans. on Control Systems Technology*, vol. 16, no. 2, pp. 297-303, 2008

[4] Y. Xu and K. W. Au, "Stabilization and path following of a single wheel robot", *IEEE/ASME Transactions on Mechatronics*, vol. 9, No. 2, pp. 407-419, June 2004

[5] J. H. Kim and S. Jung, "Development and control of a single-wheel robot", *Mechatronics*, vol. 23, pp. 594-606, 2013.

[6] S. D. Lee and S. Jung, "Experimental verification of physical relation between a gimbal system and a body system", *AIM2015*, pp. 1155-1160, 2015.

[7] S. D. Lee and S. Jung, "Experimental verification of stability region of balancing a single-wheel robot: an inverted stick model approach", *IECON 2015*, pp. 4556-4561, 2015.

[8] K. J. Astrom, B. Wittenmark, "Adaptive control." *Courier Corporation*, 2013.

[9] A. E. Bryson, "Applied optimal control: optimization, estimation and control", *CRC Press*, 1975.

[10] S. Jung, "An impedance force control approach to a quad-rotor system based on an acceleration-based disturbance observer", *Journal of Intelligent Robot Systems*, vol. 73, no. 1 , pp. 175-185, 2014.

[11] T. Murakami, F. Yu, and K. Ohnishi, "Torque sensorless control in multidegree-of-freedom manipulator", *IEEE Transactions on Industrial Electronics*, vol. 40, no. 2, pp. 259-265, 1993.

[12] E. Sariyildiz and K. Ohnishi, "On the explicit robust force control via disturbance observer", *IEEE Trans. on Industrial Electronics*, vol. 62, no. 3, pp. 1581-1589, 2015.
[13] S. Katsura, Y. Matsumoto, and K. Ohnishi, "Modeling of force sensing and validation of disturbance observer for force control", *IEEE Trans. on Industrial Electronics*, vol. 54, no.1, pp. 530-538, 2007.
[14] Y. Ohba et al., "Sensorless force control for injection molding machine using reaction torque observer considering torsion phenomenon", *IEEE Trans. on Industrial Electronics*, vol. 56, no. 8, pp. 2955-2960, 2009.
[15] S. Li, Z. Liu. "Adaptive speed control for permanent-magnet synchronous motor system with variations of load inertia", *IEEE Trans. on Industrial Electronics*, vol. 56, no. 8, pp. 3050-3059, 2009.
[16] H. S. Lee, and M. Tomizuka. "Robust motion controller design for high-accuracy positioning systems." *IEEE Trans. on Industrial Electronics*, vol. 43, no. 1, pp. 48-55, 1996.
[17] B. Yao, M. Al-Majed, and M. Tomizuka. "High-performance robust motion control of machine tools: an adaptive robust control approach and comparative experiments", *IEEE Trans. on Mechatronics*, vol. 2, no. 2, pp. 63-76, 1997.
[18] Z. J. Yang, et al. "A novel robust nonlinear motion controller with disturbance observer", *IEEE Trans. on Control Systems Technology*, vol. 16 no. 1, pp. 137-147 , 2008.
[19] K. Ohnishi, M. Shibata, T. Murakami, "Motion control for advanced mechatronics", *IEEE Trans. on Mechatronics*, vol.1, no.1, pp. 56-67, 1996.
[20] T. Umeno, Y. Hori, "Robust speed control of DC servomotors using modern two degree-of-freedom controller design", *IEEE Trans. on Industrial Electronics*, vol. 38, no. 5, pp. 363-368, 1991.
[21] A. Tesfaye, H. S. Lee, M. Tomizuka, "A sensitivity optimization approach to design of a disturbance observer in digital motion control systems", *IEEE Trans. on Mechatronics*, vol. 5, no. 1, pp. 32-38, 2000.
[22] S. D. Lee and S. Jung, “A fuzzy compensator for a single-wheel robot based on static instability.” *International Symposium on Advanced Intelligent Systems*, pp. 1203-1206, 2015.
[23] Y. Choi, K. Yang, W. K. Chung, H. R. Kim, I. H. Suh, "On the robustness and performance of disturbance observers for second-order systems", *IEEE Trans. on Automatic Control*, vol. 48, no. 2, pp. 315-320, 2003.
[24] S. D. Lee, S. Jung, "Experimental Study of finding a controllable range for self-standing motion of a single-wheel mobile robot", *Proc. of 2015 30th ICROS Annual Conference(in Korean)*, Daejeon, Korea, May 2015.